

# Design And Comparative Analysis Of An Induction Motor With Non-Oriented Electrical Steels

Chittimilla Shravan Kumar Reddy<sup>1</sup>, Dr. Ezhilarasi Arivukkannu<sup>2</sup>, Dr. Kartigeyan Jayaraman<sup>3</sup>

<sup>1</sup>Research Scholar, Dept. of EE, Annamalai University, Chidambaram, India,

[shravanreddy.eee@gmail.com](mailto:shravanreddy.eee@gmail.com), Hyderabad, Telangana, India.

<sup>2</sup>Dept. of EE, Annamalai University, Chidambaram, India. [ezhiljodhi@gmail.com](mailto:ezhiljodhi@gmail.com).

<sup>3</sup>Dept. of EEE, JBIET, Hyderabad, India. [j.kartigeyan@gmail.com](mailto:j.kartigeyan@gmail.com).

---

## ABSTRACT

The performance of an induction motor is strongly influenced by the choice of lamination steel, as magnetic properties directly affect iron losses and overall efficiency. In this study, a three-phase, 5 HP 50 Hz squirrel-cage induction motor was designed and analysed using ANSYS Electronics Desktop, with the initial design performed in RMXprt and detailed simulations carried out in Maxwell 2D/3D. Three grades of non-oriented electrical steel DI-MAX series (M15, M19, and M36) were evaluated under identical motor geometry and operating conditions. The investigation focused on core loss distribution and efficiency at rated load, as these parameters directly reflect the impact of the lamination material. The results show that M19 exhibited the best performance, with the lowest total core loss of 5 W (4 W in the stator and 0.5 W in the rotor) and the highest efficiency of 92.33%. The motor using M15 recorded moderate performance, with 16 W of core loss (15 W stator, 1 W rotor) and an efficiency of 91.47%. In contrast, M36 resulted in the highest core losses of 40 W (38 W stator, 2 W rotor), leading to the lowest efficiency of 90.14%. These findings confirm that the selection of lamination steel plays a decisive role in energy efficiency and loss minimization. The study demonstrates that advanced simulation tools can effectively guide material selection for induction motor design, where M19 emerges as the most suitable option, while M15 offers a compromise between performance and cost.

**Keywords:** Induction Motor, Electrical Machine Simulation, ANSYS, Stator, Non-Oriented Electrical steel, Core Loss, Efficiency.

---

## 1. INTRODUCTION

Induction motors are the most widely used type of electrical machines because of their rugged construction, low cost, and ability to operate with minimum maintenance. They are employed in industries, commercial installations, and domestic applications, which makes them a major consumer of electrical energy. Studies indicate that more than half of the electrical energy generated worldwide is consumed by electric motors, out of which induction motors form a substantial portion[4]. In this context, even a small improvement in efficiency at the individual machine level leads to considerable energy savings at the system level. The overall performance of an induction motor is influenced by various losses, of which the core loss is particularly significant[7]. Core loss is determined by the magnetic properties of the lamination material used in the stator and rotor. It can be expressed as the sum of hysteresis and eddy current losses:

$$P_c = P_h + P_e$$

Hysteresis loss is proportional to frequency and the Steinmetz law,

$$P_h = K_h f B_{max}^n V$$

where  $f$  is the frequency,  $B_{max}$  is the maximum flux density,  $n$  is the Steinmetz exponent, and  $V$  is the core volume. Eddy current loss, on the other hand, depends on the square of frequency and the square of lamination thickness:

$$P_e = K_e f^2 B_{max}^2 t^2 V$$

where  $t$  is the lamination thickness. These relations explain why the grade and thickness of electrical steel have a direct effect on the iron losses of a machine. The choice of material also influences the efficiency of the motor, which is defined as:

$$\eta = \frac{P_{out}}{P_{in}} \times 100$$

where the input power  $P_{in}$  is given by:

$$P_{in} = \sqrt{3} V_{ph} I_{ph} \cos \phi$$

and the output power  $P_{out}$  is the net power developed after subtracting copper and core losses from the input. The reduction of iron losses through the use of improved lamination steels therefore directly enhances machine efficiency[10]. In addition, the air-gap torque is related to the air-gap power and synchronous speed as:

$$T = \frac{P_g}{\omega_s}, \quad P_g = P_{in} - (P_{stator\_cu} + P_c)$$

where  $\omega_s$  is the synchronous angular speed. Similarly, the power factor of the machine is determined by:

$$\cos\phi = \frac{P_{in}}{\sqrt{3}V_{ph}I_{ph}}$$

and depends on the magnetizing current, which in turn is affected by the permeability of the lamination steel.

Although several studies have been conducted on the design and optimization of induction motors, there are only limited reports that systematically compare the performance of different non-oriented electrical steels using modern simulation tools. In particular, the DI-MAX series, consisting of grades such as M15, M19, and M36, is widely used in practice but has not been extensively compared in a single design framework.

The present work aims to fill this gap by designing and analyzing a three-phase, 5 HP, 50 Hz squirrel-cage induction motor using ANSYS Electronics Desktop. The preliminary design was performed using RMxpert, while detailed electromagnetic analysis was carried out using Maxwell 2D/3D. The influence of lamination material was studied by keeping the geometry and winding constant, and only the steel grade was varied. The focus of the study is on core loss distribution, efficiency, torque-speed characteristics, and power factor behavior, in order to identify the most suitable lamination material for small and medium rating induction motors.

## 2. METHOD

The methodology adopted for this work consists of four major stages: motor specification, preliminary design, finite element simulation, and performance evaluation[14]. Each stage was carried out in a systematic manner to ensure accuracy and reliability of results. A three-phase, 5 HP squirrel cage induction motor operating at 50 Hz supply frequency was considered for the study. The key design inputs such as rated power, supply voltage, number of poles, synchronous speed, and connection type were fixed as per standard industrial practice. The main focus of the investigation was to study the impact of different grades of electrical steel laminations DI-MAX series M15, M19 and M36 on the motor performance[16]. These materials are widely used in electrical machines but differ in terms of magnetic properties and loss characteristics. Hence, their selection plays a vital role in deciding efficiency, torque capability, and overall performance of the motor. The initial stage of modeling was carried out using ANSYS RMxpert, a specialized tool for electric machine design. After entering the basic specifications of the motor, the software generated an equivalent circuit representation of the induction motor[18]. This model provided key electrical parameters such as stator resistance, rotor resistance, leakage reactance, and magnetizing reactance. The software also predicted preliminary performance values including torque, efficiency, and power factor. Separate designs were created for each lamination material, and the results were noted for comparison. The main purpose of this stage was to obtain a quick and reliable estimation of the motor characteristics before proceeding to detailed analysis[20]. For a more accurate study, the RMxpert models were exported to ANSYS Maxwell, which uses finite element analysis to simulate electromagnetic fields. A detailed 2D cross-sectional geometry of the motor was generated, and meshing was applied to divide the geometry into small elements for precise calculations. Boundary conditions were carefully assigned to represent realistic operating conditions of the motor. The simulations carried out in Maxwell provided valuable results such as flux distribution in the core, air-gap flux density, torque generation, efficiency, and core losses. Since lamination material directly affects hysteresis and eddy current losses, this stage allowed a deeper understanding of how DI-MAX series M15, M19, and M36 behave under identical operating conditions. The results obtained from this analysis are considered more accurate compared to equivalent circuit predictions. The data obtained from Maxwell simulations were systematically compared for the three materials. Parameters such as efficiency, torque-speed characteristics, power factor, and core losses were examined in detail. Graphs and tables were prepared to present the variation in performance due to the choice of lamination. From the analysis, it was observed that high-grade materials such as DI-MAX-M15 reduced core losses and improved efficiency, while lower grades like DI-MAX-M36 increased

the losses but offered cost advantages. Thus, the final evaluation highlights the trade-off between efficiency and economy, and provides guidelines for selecting the appropriate lamination grade depending on application requirements.

### 3. Design of Induction motor

This work uses a simulation-based test rig built in Ansys Electronics Desktop to study how non-oriented electrical steels DI-MAX series M15, M19 and M36 influence the performance of a three-phase, 5 HP induction motor. The geometry, winding and operating conditions are kept identical across all cases; only the core lamination material is varied for the stator and the rotor. The induction motor was designed using ANSYS RMxpert for preliminary modeling and parameter estimation. The model was then exported to ANSYS Maxwell 2D/3D for detailed finite element analysis. The DI-MAX series non-oriented electrical steel grades M15, M19 and M36 are applied to both stator and rotor laminations in three separate designs. All other inputs including slots, coils, current and boundary settings remain unchanged to ensure a fair comparison that isolates material effects on hysteresis and eddy current loss. Motor geometry, winding, and operating conditions were kept constant for all cases. Only the lamination material DI-MAX series M15, M19, and M36 was varied to study its effect on performance. Key results such as flux distribution, core losses, torque-speed, and efficiency were obtained for comparison.

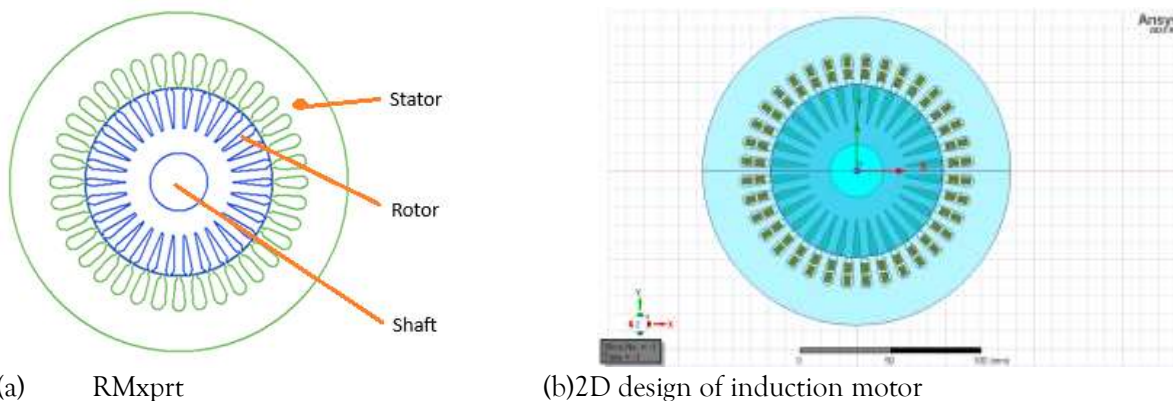


Figure 3.1 Geometrical models of Induction motor using RMxpert and 2D Maxwell  
Table 3.1 Motor specifications common to all materials

Parameter	Value
Rated power	5 HP, 3.72 kW
Supply	400 V, three phase, 50 Hz, '
Poles	4
Synchronous speed	1500 rpm
Rated speed	about 1450–1470 rpm
Stator slots	36
Rotor slots	30
Mechanical air-gap	0.25 mm
Stator OD	173.5 mm
Stator ID	97.2 mm
Rotor ID	30 mm
Stack length	137 mm
Winding	Double-layer, whole-coiled
Turns per phase	204

## 4. DISCUSSION AND COMPARATIVE ANALYSIS

### A. Efficiency vs Speed

Across the full speed range, all three motors follow the expected rise in efficiency from low speed to near-rated speed, with a slight roll-off toward synchronous speed. At ~1,450 to 1,470 rpm, the DI-MAX-M19 build is clearly on top, followed by DI-MAX-M15, with DI-MAX-M36 lowest. At the rated operating point, the efficiencies obtained were approximately 91.5% for M15, 92.33% for M19, and 90.14% for M36, following the same order as their core-loss values. The efficiency profile of M19 rises more quickly and

sustains a broad plateau around the rated speed, which reflects its lower magnetizing requirements and improved iron-loss performance under identical design and loading conditions.

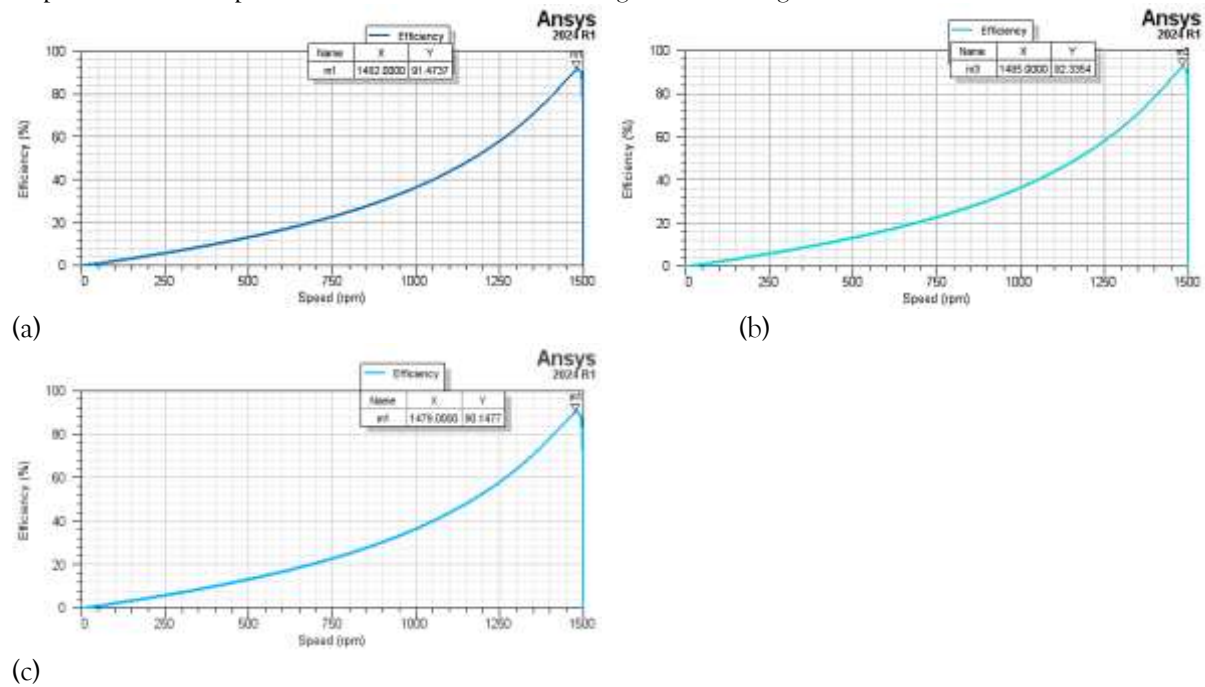


Figure 4.1: Efficiency vs Speed graphs (a) M15 (b) M19 (c) M36

#### B. Torque – Speed Characteristics

The torque-speed characteristics for the three grades of non-oriented electrical steel, namely DI-MAX series M15, M19, and M36, are shown in Figure 4.2. In all the cases, torque gradually increases with speed and reaches a maximum value before the rated speed. For M15, the peak torque obtained is around 83.9 Nm at 1185 rpm. In the case of M19, the maximum torque rises slightly higher to about 84.0 Nm at the same speed. For M36, the torque value reduces to approximately 82.7 Nm at 1185 rpm. Beyond this point, all three curves drop sharply as the motor approaches synchronous speed, showing the typical characteristic of induction motors. The comparison reveals that M19 provides the highest torque among the three grades, making it the best choice in terms of torque performance. Overall, M19 stands out as the most suitable material for achieving better torque output and efficiency.

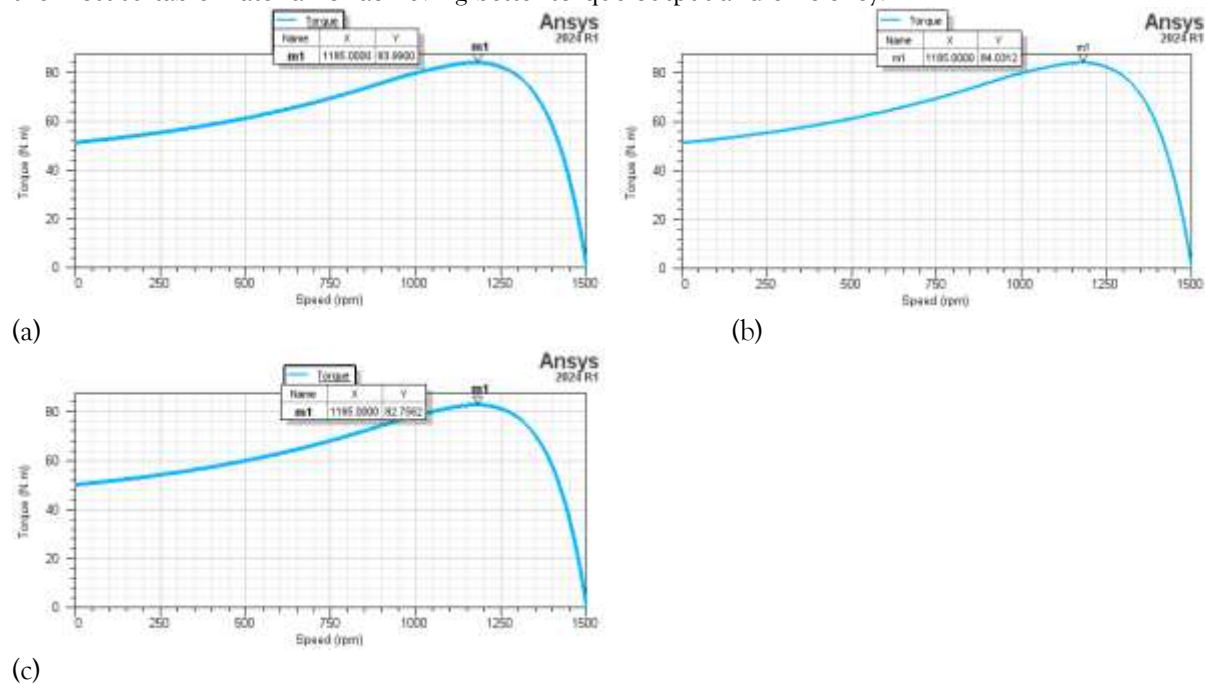


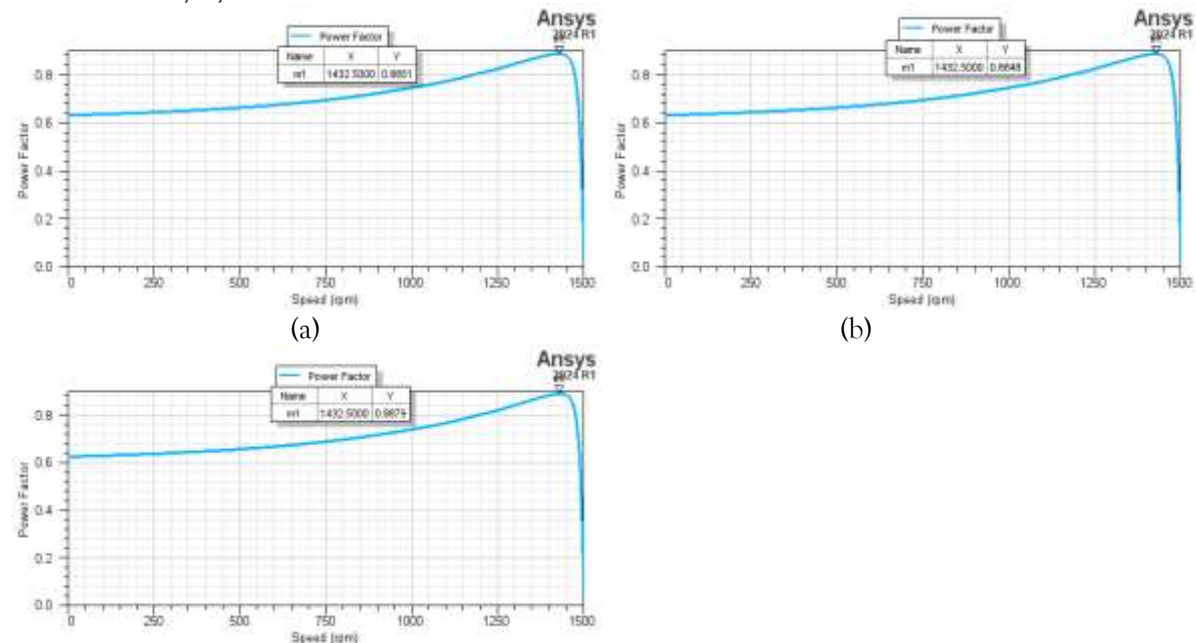
Figure 4.2: Torque vs Speed graphs (a) M15 (b) M19 (c) M36

#### C. Power Factor vs Speed

The variation of power factor with speed for three grades of non-oriented electrical steel DI-MAX series M15, M19, and M36 is presented in Figure 4.3. In all three cases, the power factor increases gradually



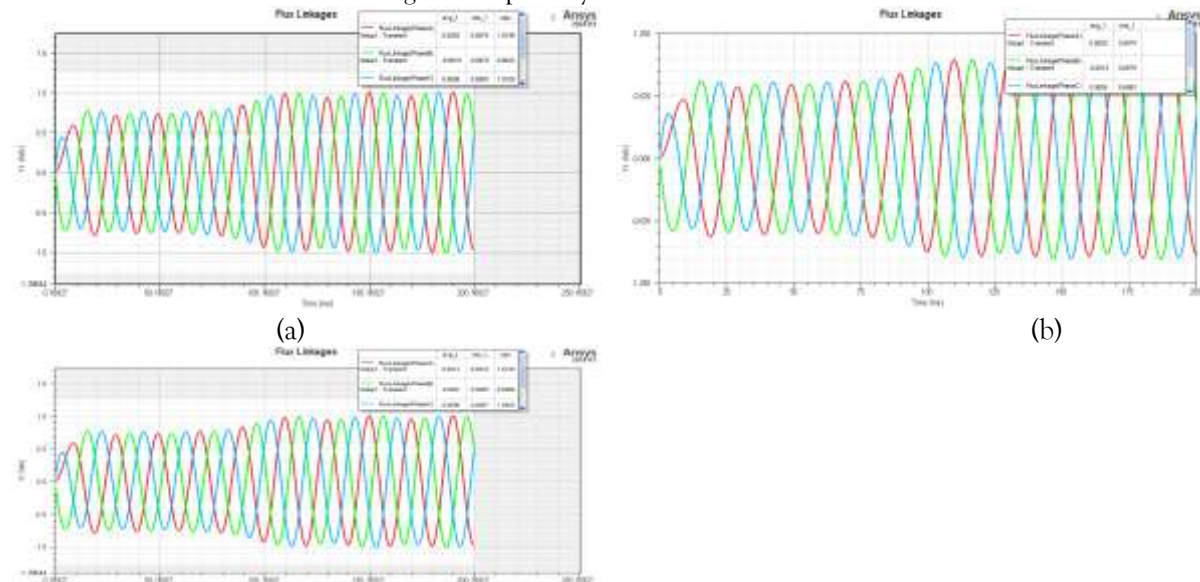
with speed and reaches its maximum value near the rated speed. For M15, the peak power factor is about 0.885 at 1432 rpm. In the case of M19, the maximum value slightly improves to 0.884, while M36 shows a still better value of 0.887 at the same operating speed. This indicates that M36 provides the highest power factor, which helps in reducing reactive power and improving efficiency. The curves also show that at lower speeds, the power factor remains low and then rises steadily as the motor approaches synchronous speed. Comparing the results, M36 stands out as the best material in terms of power factor performance, followed closely by M19 and M15.



(c)  
Figure 4.3: Power factor vs speed (a) M15 (b) M19 (c) M36

#### D. Flux Linkages

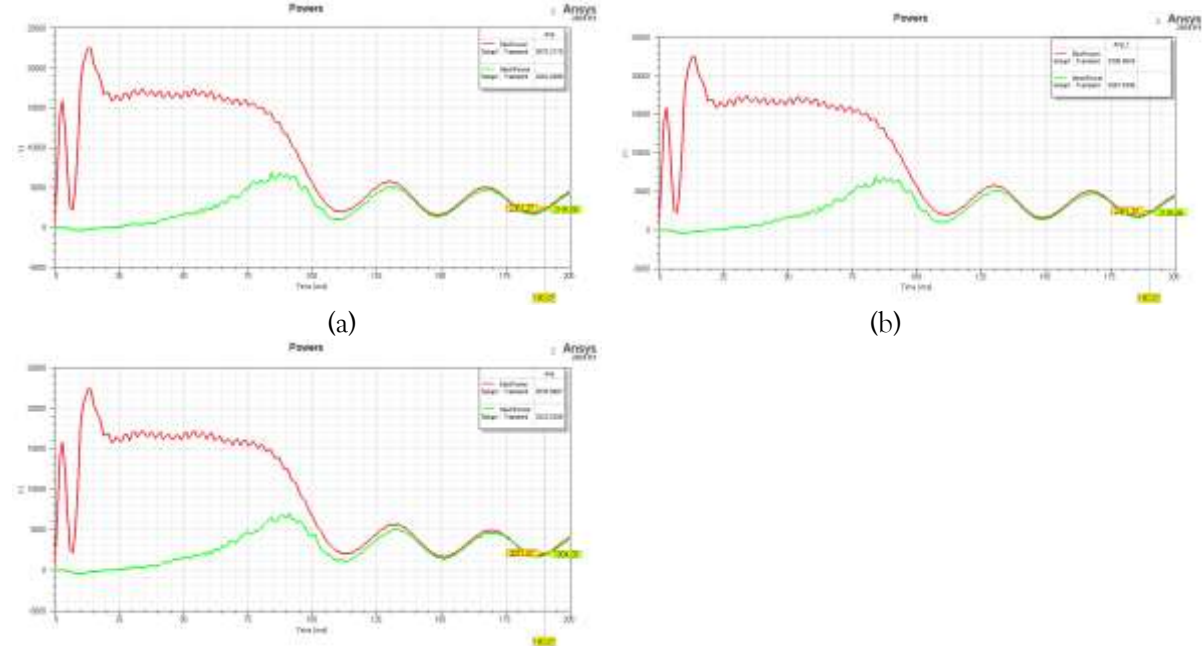
The flux linkage characteristics of the induction motor using DI-MAX series M15, M19, and M36 grades of electrical steel are shown in Figure 4.4. The waveforms represent the flux linkages in the three phases, which vary sinusoidally with time. For M15, the maximum flux linkage reaches around 1.02 Wb, while M19 shows a slightly reduced peak of about 0.99 Wb. In the case of M36, the flux linkage further decreases to nearly 0.96 Wb. The results indicate that M15 maintains higher flux linkage compared to M19 and M36, which contributes to better magnetic performance. Although all three materials show balanced and symmetrical waveforms, the amplitude clearly differentiates their effectiveness. From the comparison, it is evident that M15 provides the strongest flux linkage, making it the best choice among the three materials in terms of magnetic capability.



(c)  
Figure 4.4: Flux linkages (a) M15 (b) M19 (c) M36

### E. Powers vs Time

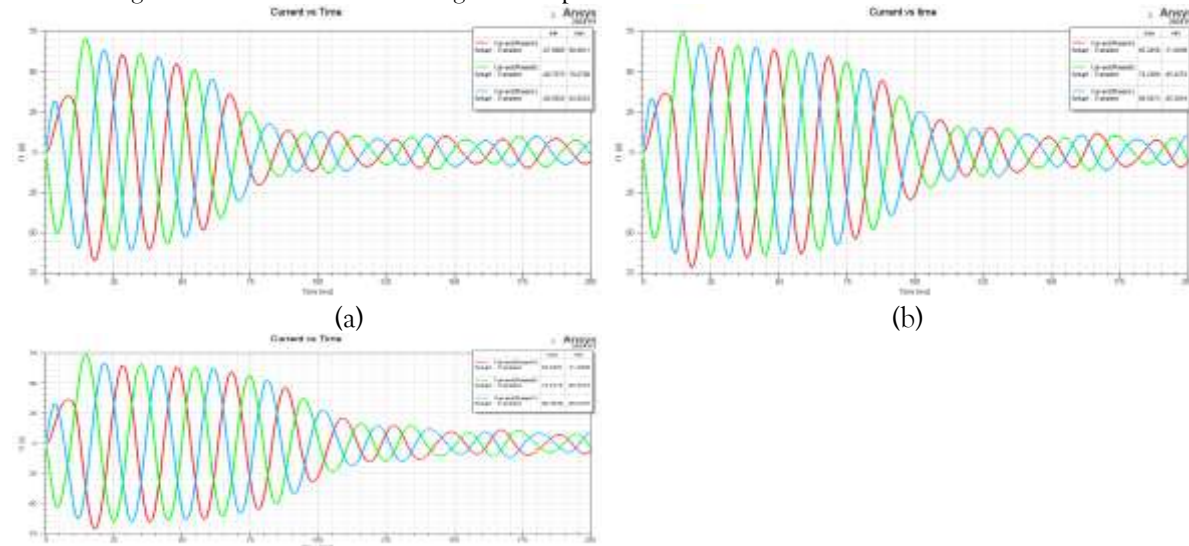
The power versus time plots for DI-MAX series M15, M19, and M36 show clear differences in performance. From Fig 4.5(a), M15 the maximum input power reaches around 19,970 W, while the output stabilizes near 10,820 W. In the case of M19 in the Fig 4.5(b), the peak input is about 19,963 W, with output power settling close to 10,817 W. For M36, the maximum recorded input is around 19,957 W, and the output stabilizes near 10,810 W shown in Fig 4.5(c). The curves reveal that all three materials experience initial power surges followed by oscillations before reaching steady state. Among them, M36 shows slightly higher losses, while M19 performs moderately. M15 records marginally better efficiency with lower losses. Hence, M15 is the best material in terms of power handling and efficiency.



(c)  
Figure 4.5: Powers vs Time (a) M15 (b) M19 (c) M36

### F. Current vs Time

The plots represent current versus time for DI-MAX series of M15, M19, and M36 materials. From Fig.6(a), M15 the peak current reaches about 68.47 A, later decaying smoothly to a steady value of around 22.98 A. In the case of M19 in the Fig.6(b), the maximum current is about 68.56 A, settling near 22.95 A after damping. From Fig.6(c), M36 the initial peak is slightly higher at 68.61 A, and the steady-state value is approximately 22.89 A. The oscillations in all three gradually decrease, showing system stability. Among them, M36 has the highest initial current stress, while M15 shows slightly lower values. The reduced steady-state current in M15 indicates better efficiency. Hence, M15 is the best material for minimizing current losses and ensuring stable operation.



(c)  
Figure 4.6: Current vs Time (a) M15 (b) M19 (c) M36

## G. Core Loss

The core loss distribution in M15, M19, and M36 includes both stator core loss and rotor core loss caused by hysteresis and eddy currents. From Fig.4.7 (a), M15 the total core loss peaks at 41.02 W with an average of 14.89 W, showing lower loss in both stator and rotor cores. From Fig.4.7 (b), M19 the maximum loss is 37.50 W and the average is 13.61 W, where the stator core contributes slightly more than the rotor core. From Fig.4.7 (c), M36 losses are much higher, peaking at 79.12 W with an average of 28.93 W, which indicates significant energy wastage in both stator and rotor cores. The high rotor losses in M36 can lead to excessive heating, while the stator losses further reduce efficiency. Comparing all three, M36 is least efficient, M19 gives moderate results, and M15 shows the best balance. Hence, M15 is the most suitable material for minimizing stator and rotor core losses and improving machine efficiency.

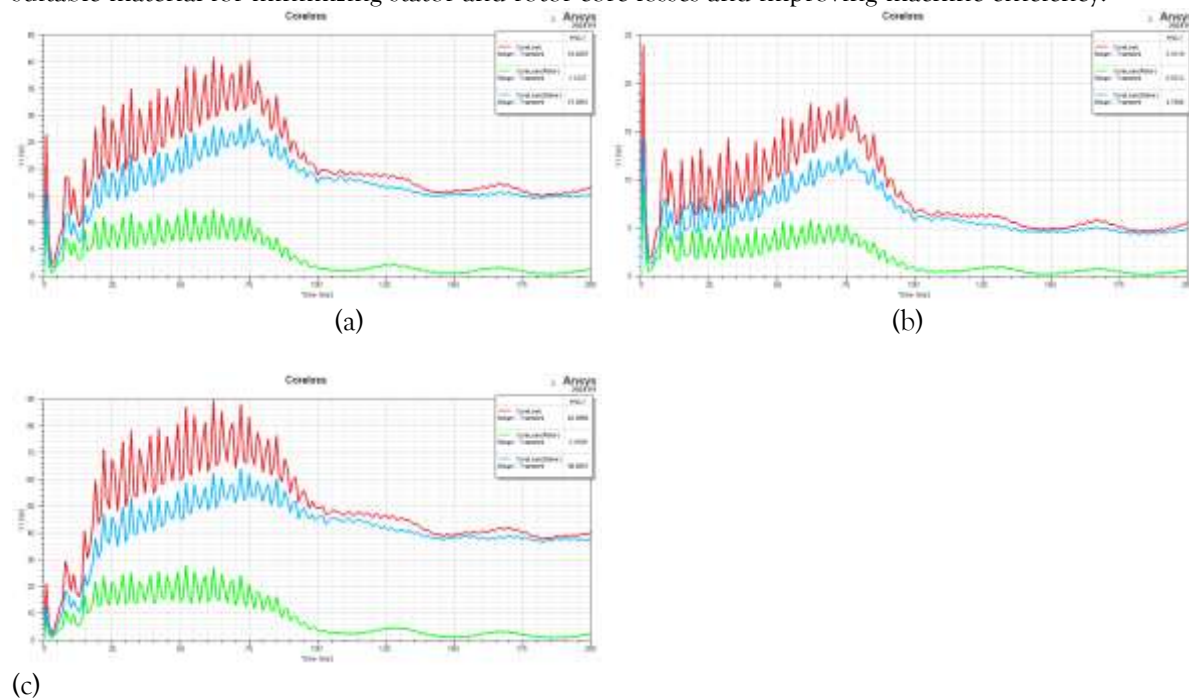


Figure 4.7: Core loss (a) M15 (b) M19 (c) M36

## 5. CONCLUSION

The comparative study of M15, M19, and M36 laminated induction motors highlights the significant influence of core material on overall performance. Among the three, M19 consistently achieved the best results with an efficiency of 92.3%, the lowest core loss of 5 W, and the highest power factor of approximately 0.90. M15 demonstrated moderate efficiency of 91.5% with reasonably balanced performance, whereas M36 exhibited the highest core losses of 40 W and the lowest efficiency of 90.1%. The torque-speed and current-power characteristics further confirmed that M19 delivers more stable torque with reduced current demand compared to the other two materials. Based on these findings, M19 can be considered the most suitable lamination steel, with M15 serving as a cost-effective compromise, while M36 is least preferred due to its poor efficiency and higher losses.



## REFERENCES:

- [1] P.B. Reddy, A.M. El-Refai, S. Galioto, J.P. Alexander, Design of synchronous reluctance motor utilizing dual-phase material for traction applications, *IEEE Trans. Ind. Appl.* 53 (3) (2017) 1948–1957.
- [2] J. Zhu, K.W.E. Cheng, X. Xue, Y. Zou, Design of a new enhanced torque in-wheel switched reluctance motor with divided teeth for electric vehicles, *IEEE Trans. Magn.* 53 (11) (2017) 1–4.
- [3] C.C. Chan, A. Bouscayrol, K. Chen, Electric, hybrid, and fuel-cell vehicles: architectures and modeling, *IEEE Trans. Veh. Technol.* 59 (2) (2009) 589–598.
- [4] J. Mei, Y. Zuo, C.H. Lee, J.L. Kirtley, Modeling and optimizing method for axial flux induction motor of electric vehicles, *IEEE Trans. Veh. Technol.* 69 (11) (2020) 12822–12831.
- [5] G. Singh, T.C.A. Kumar, V. Naikan, Induction motor inter turn fault detection using infrared thermographic analysis, *Infrared Phys. Technol.* 77 (2016) 277–282.
- [6] A. Boglietti, A. Cavagnino, M. Lazzari, S. Vaschetto, Preliminary induction motor electromagnetic sizing based on a geometrical approach, *IET Electr. Power Appl.* 6 (9) (2012) 583–592.
- [7] M.J. Akhtar, R.K. Behera, Optimal design of stator and rotor slot of induction motor for electric vehicle applications, *IET Electr. Syst. Transp.* 9 (1) (2019) 35–43.




- [8] D.F. de Souza, F.A.M. Salotti, I.L. Sauer, H. Tatizawa, A.T. de Almeida, A. G. Kanashiro, A performance evaluation of three-phase induction electric motors between 1945 and 2020, *Energies* 15 (6) (2022) 2002.
- [9] E. El-Kharashi, "Design and predicting efficiency of highly nonlinear hollow cylinders switched reluctance motor," *Energy Conversion and Management*, vol. 48, no. 8, pp. 2261–2275, 2007, doi: 10.1016/j.enconman.2007.04.006.
- [10] A. Parsapour, B. M. Dehkordi, and M. Moallem, "Predicting core losses and efficiency of SRM in continuous current mode of operation using improved analytical technique," *Journal of Magnetism and Magnetic Materials*, vol. 378, pp. 118–127, 2015, doi: 10.1016/j.jmmm.2014.10.148.
- [11] K. Chwastek, "Anisotropic properties of non-oriented steel sheets," *IET Electric Power Applications*, vol. 7, no. 7, pp. 575–579, 2013, doi: 10.1049/iet-epa.2013.0087.
- [12] C. H. S. K. Reddy, M. Ramaswamy, and K. Jayaraman, "Investigative study on the properties of magnetic materials for electrical machines," *Indonesian Journal of Electrical Engineering and Computer Science*, vol. 32, no. 1, pp. 71–79, 2023, doi: 10.11591/ijeecs.v32.i1.pp71-79.
- [13] N. Susmitha, T. Revanth, S. A. Reddy, and P. S. Rani, "Performance analysis of induction motor using ansys," *International Journal of Innovative Technology and Exploring Engineering*, vol. 9, no. 6, 2020, doi: 10.35940/ijitee.F4556.049620.
- [14] M. Aishwarya and R. M. Brisilla, "Design of energy-efficient induction motor using ANSYS software," *Results in Engineering*, vol. 16, 2022, doi: 10.1016/j.rineng.2022.100616.
- [15] D. T. Peters, J. G. Cowie, E. F. Brush, and D. J. Van Son, "Copper in the squirrel cage for improved motor performance," in *IEEE International Electric Machines and Drives Conference (IEMDC)*, 2003, pp. 1265–1271, doi: 10.1109/IEMDC.2003.1210402.
- [16] J. Kartigeyan and M. Ramaswamy, "Effect of material properties on core loss in switched reluctance motor using non-oriented electrical steels," *Journal of Magnetism*, vol. 22, pp. 93–99, 2017, doi: 10.4283/JMAG.2017.22.1.093.
- [17] J. S. M. Pedrosa, S. D. C. Paolinelli, and A. B. Cota, "Influence of initial annealing on structure evolution and magnetic properties of 3.4% Si non-oriented steel during final annealing," *Journal of Magnetism and Magnetic Materials*, vol. 393, pp. 146–150, Nov. 2015, doi: 10.1016/j.jmmm.2015.05.058.
- [18] M. Tietz, P. Biele, A. Jansen, F. Herget, K. Telger, and K. Hameyer, "Application-specific development of non-oriented electrical steel for EV traction drives," in *2012 2nd International Electric Drives Production Conference, EDPC 2012 - Proceedings*, Oct. 2012, pp. 1–5, doi: 10.1109/EDPC.2012.6425126.
- [19] K. Anumala and R. B. Veligatla, "Novel axial flux machines topology assessment and their feasible applications," *International Journal of Power Electronics and Drive Systems (IJPEDS)*, vol. 13, no. 1, pp. 84–92, 2022, doi: 10.11591/ijpeds.v13.i1.pp84-92.
- [20] C. H. S. K. Reddy, Ezhilarasi Arivukkannu, and K. Jayaraman, "Performance comparison of core loss in induction motor using non-oriented electrical steels" *International Journal of Applied Power Engineering (IJAPE)*, Vol. 14, No. 3, September 2025, pp. 640–646, doi: 10.11591/ijape.v14.i3.pp640-646 .
- [21] N. Aisyah, M. Azri, A. Jidin, and M. Z. Aihsan, "A new optimal direct torque control switching strategy for open-end windings induction machine using a dual-inverter," *International Journal of Power Electronics and Drive Systems (IJPEDS)*, vol. 12, no. 3, pp. 1405–1412, Sep. 2021, doi: 10.11591/ijpeds.v12.i3.pp1405-1412.

## BIOGRAPHIES OF AUTHOR

	<p><b>Chittimilla Shravan Kumar Reddy</b> is a research scholar in Electrical Engineering at Annamalai University. He earned his B.Tech in Electrical and Electronics Engineering (EEE) in 2011 from Joginpally B. R Engineering College, JNTU Hyderabad, and his M.Tech in Power Electronics and Electric Drives from the same institution. Currently, he serves as an Assistant Professor at J.B Institute of Engineering and Technology. His primary research interests are in the areas of Electrical Machines and Power Electronics. He can be reached via email: <a href="mailto:shravanreddy.eee@gmail.com">shravanreddy.eee@gmail.com</a></p>
	<p><b>Dr. A. Ezhilarasi</b> obtained her bachelor's degree in Electrical and Electronics Engineering, her master's degree in Power Systems Engineering, and her Ph.D. in Electrical Engineering from Annamalai University, Chidambaram, India, in 1998, 2005, and 2013, respectively. With more than 24 years of teaching experience, she has held several positions and currently serves as an Associate Professor in the Department of Electrical Engineering at Annamalai University. Her research focuses on the design, modeling, analysis, and development of various power electronic converters, with a particular emphasis on new control schemes aimed at improving performance. Her work has been published in numerous peer-reviewed international journals. Her areas of interest include power</p>



	<p>electronics, solid-state drives, and intelligent control techniques. She can be contacted via email at <a href="mailto:ezhiljodhi@gmail.com">ezhiljodhi@gmail.com</a>. Contact No: 9442866160</p>
	<p><b>Dr. Kartigeyan Jayaraman</b> earned his Bachelor's degree in Electrical and Electronics Engineering from Madras University in 2004, his Master's degree in Electrical Drives and Control from Pondicherry University in 2007, and his Doctoral degree in Electrical Engineering from Annamalai University in 2017. He is currently serving as an Associate Professor in the Department of Electrical and Electronics Engineering and as Dean of Student Affairs at J.B. Institute of Engineering and Technology, Hyderabad, India. With numerous publications in both National and International journals, his research interests include core loss modeling, magnetic materials, and the design and control of switched reluctance and AC machines. He can be contacted via email: <a href="mailto:j.kartigeyan@gmail.com">j.kartigeyan@gmail.com</a>.</p>